

Quantitative Analysis of IR Intensities of Alkanes Adsorbed on Solid Acid Catalysts

Friederike C. Jentoft,^{1} Jutta Kröhnert,¹ Irina R. Subbotina,² Vladimir B. Kazansky²*

¹ Department of Inorganic Chemistry, Fritz-Haber-Institut der Max-Planck-Gesellschaft
Faradayweg 4-6, 14195 Berlin (Dahlem), Germany

² N.D. Zelinsky Institute of Organic Chemistry, Russian Academy of Sciences
Leninsky Prospect 47, Moscow 117913, Russia

*corresponding author, new address: School of Chemical, Biological and Materials Engineering,
University of Oklahoma, Norman, OK 73019, USA, email: fcjentoft@ou.edu

Abstract

The goal of this work was to determine the integrated molar absorption coefficients of adsorbate vibrations and to use them as a measure of the activation of chemical bonds by the catalyst surface. For this purpose, an apparatus was built for the simultaneous measurement of transmission IR spectra of the adsorbate and the corresponding adsorption isotherm; the adsorbed amount was determined by a volumetric–barometric method. The adsorption of *n*-butane and 2,2-dimethylpropane on self-supporting wafers of mordenite and sulfated zirconia samples was investigated at temperatures of 298–308 K and alkane pressures of 0–100 hPa. The linear range of plots of the IR band intensities vs. coverage was used to determine absorption coefficients of C–H stretching vibrations. The coefficients were found to depend on particle size and morphology, and it is shown that they are overestimated because the pathlength is enhanced through strong scattering in the wafers. The results reveal the limitations of quantitative analysis by transmission IR spectra when fine powders (such as catalysts) are investigated.

Keywords: zeolite, mordenite, sulfated zirconia, 2,2-dimethyl propane, FTIR spectroscopy, absorption coefficient, adsorption, catalysis, scattering, neopentane

Introduction

In heterogeneous catalysis it is of paramount importance to understand the transformation of a molecule through adsorption and subsequent conversion on a surface. Adsorption experiments are frequently used to characterize specific sites on surfaces; probe molecules can be selected such that they adsorb preferentially on acidic, basic, or metal sites. A combination of methods is necessary to determine the nature of the adsorbate, the number of sites, the accessibility of the sites, as well as kinetic and thermodynamic parameters of the adsorption such as activation energies and heats of adsorption. A quantitative measure of the strength of interaction between a molecule and the surface is the heat that evolves, which, however, will not reveal specific changes to the chemical bonds of the molecule and the surface functional groups. The structure of the adsorbate is expressed in its vibrational signature, which can be revealed by IR spectroscopy. Typically, shifts of vibrations of the adsorbate relative to the gas phase frequencies or shifts of vibrations of surface functional groups are analyzed. With the help of such band shifts, samples and sites can be compared; for example, the position of the CO vibration correlates with the electric field strength of the metal cation adsorption site,¹ and the shift of surface OH group vibrations upon CO adsorption depends on the protonic acidity.² However, the IR spectrum contains more information, namely in the absolute band intensities and shapes, whose potential in describing the interactions between the surface and an adsorbed species still remains to be fully exploited.

From a theoretical point of view, band intensities in IR spectra are intriguing. The intensity depends on the change of the dipole moment during the vibration, which reflects the polarization of a bond during the vibration. In a chemical transformation involving a heterolytic bond cleavage, polarization of a bond represents the onset of a reaction. The dynamic dipole moment of a specific vibration in a free or adsorbed molecule, which is represented by the IR intensity,

could be a measure of the reactivity of the associated bond. Indeed, it has been attempted to use the C–H stretching band intensity to evaluate the protonic acidity in free hydrocarbon molecules.³ The IR intensity distribution obtained for a free molecule in the gas phase can serve as a reference point when considering the effect of a catalyst surface on the molecule. With respect to catalysis, it would be interesting to determine which bonds within a molecule are being activated in order to predict selectivities, and also to assess the extent of the activation of these individual bonds. A simple qualitative experiment is to compare intensity distributions in spectra representing the free and the adsorbed state. Our recent work shows considerable changes in the intensity distribution of hydrocarbon vibrations upon adsorption on zeolites and other oxidic surfaces, and significant variations in the adsorbate spectra depending on the adsorption site.⁴⁻⁷ For example, the relative intensity of the symmetric vibration of methane, which becomes visible after adsorption, varies with the zeolite framework type and the nature of the cation in the zeolite.⁴

Relative intensities in adsorbate spectra, which are easily evaluated, do not necessarily indicate which vibrations have become more or less intense through interaction of the molecule with the catalyst. Molar IR absorption coefficients have to be determined and, therefore, a second independent method is required to deliver information on how many vibrating molecules (oscillators) contribute to the intensity of a particular band. Semi-quantitative attempts have been made by Risse et al.⁸ who used a concurrent temperature-programmed desorption experiment to estimate relative oscillator strengths of adsorbed CO. Platon and Thomson⁹ employed diffuse reflectance IR spectroscopy to obtain a ratio of the molar absorption coefficients for pyridine adsorbed on Lewis or Brønsted acid sites, respectively. Absolute intensities have been evaluated by applying transmission IR spectroscopy. The adsorbed amount has been determined by assuming complete adsorption of a known dose of probe molecule,^{10,11} by separate

gravimetric^{12,13,14} or volumetric experiments,¹⁵ or by simultaneous gravimetric measurements.^{14,16,17} However, some of the described procedures will not work when adsorption is incomplete (because of weak interaction) and some are not sensitive enough to work at low coverages, which might be desirable if only a fraction of sites on a heterogeneous surface is to be populated and investigated.

The goal of this work was, first, to develop an apparatus to measure the adsorbed amount and the corresponding spectra simultaneously, and then to use this data to determine molar absorption coefficients for selected vibrations of adsorbates on catalyst surfaces. The selected scientific problem is the activation of alkanes on the surface of solid acids, which occurs at much lower temperature on sulfated zirconia^{18,19} than on zeolites such as H-mordenite.^{19,20} This behavior could not be explained by the acidic properties of these materials,²¹ and investigation of the adsorption of alkanes may provide new insight into this matter. *n*-Butane was chosen as an adsorptive to connect to published data and validate measurements; however, *n*-butane reacts already at room temperature on sulfated zirconia and is not suitable to determine molar absorption coefficients. 2,2-Dimethylpropane (neopentane) was selected for this purpose; on sulfated zirconia, it is converted in significant amounts only above a temperature of 573 K.²²

Experimental methods

Materials and characterization

Sulfated zirconia (SZ) was produced through 3 h calcination of sulfated hydrous zirconia (MEL XZO 681) at 823 K. Iron was introduced to the same raw material through the incipient wetness method followed by calcination at 923 K (FeSZ). The batch size used for calcination was varied between 3 g (suffix “SB”), 10–12 g (“MB”), and 20–25 g (“LB”), with Arabic numerals 1 and 2 indicating repeat preparations using the same batch size. Details can be found in Refs. ^{23,24}.

Two different mordenite samples in hydrogen form, with Si/Al = 17 (HMOR I) and 20 (HMOR II), were kindly provided by F. Fetting (TU Darmstadt) and J.A. Lercher (TU München). Scanning electron microscopy (SEM) images were taken with a Hitachi S-4000 with a field emission gun at an acceleration voltage of 2 kV.

n-Butane and 2,2-dimethyl propane were of 99.5 and 99 % purity (Messer), respectively, and were further dried with Hydrosorb cartridges (Messer).

Volumetric-barometric apparatus and calibration

A custom-made vacuum and gas dosing apparatus, which includes a heatable section for sample pretreatment and a section with KBr windows, was used to measure adsorption isotherms. Pressure measurement was performed with absolute pressure transducers (MKS Baratron). The gas dosing part is encased in a plastic box with a forced air heater for temperature control. “Box temperature” refers to this compartment. The entire gas dosing system comprises three compartments, the sample cell volume V_{sc} , the dosing volume V_{dos} , and the calibration volume V_{cal} . The calibration volume consists of a glass body and an all-metal CF 16 corner valve. The size of this volume was determined by measuring the amount of water that it can contain; the result was 29.46 ml.

V_{sc} and V_{dos} together are called the total volume V_{tot} . V_{tot} can be determined by a series of experiments in which V_{tot} is filled to a certain pressure and then the gas is expanded into the previously evacuated V_{cal} . For each pair of pressures p_{tot} and $p_{tot+cal}$ a value of V_{tot} is obtained using Eq. 1:

$$V_{tot} = \frac{p_{tot+cal}}{p_{tot} - p_{tot+cal}} V_{cal} \quad (1)$$

V_{tot} was determined to 373 ± 2 ml. Furthermore, from a series of experiments with varying pressure, an expansion factor is obtained for the expansion of gas from V_{dos} into V_{tot} :

$$f = \frac{P_{dos}}{P_{tot}} \quad (2)$$

This factor was determined to be 0.813 ± 0.001 .

Combined adsorption and spectroscopic experiment

The powders were pressed into self-supporting wafers by applying pressures between 98.4 and 123 MPa. The pellets, which weighed between 4.7 and 47.2 mg cm⁻², were introduced in the apparatus and activated for 1.5 h at 723 K in vacuum (final pressure < 2*10⁻⁶ hPa); heating and cooling rates were 7 K min⁻¹. The gas was introduced stepwise by expanding from V_{dos} into V_{tot} . The sample could be placed in or out of the beam, and pressures were recorded after the adsorption equilibrium was established. The amount adsorbed on the sample in the i^{th} dosing step, $n_{ads,i}$, was calculated using Eq. 3:

$$n_{ads,i} = ((p_{dos,i} - p_{tot,i-1})f + p_{tot,i-1} - p_{tot,i}) \frac{V_{tot}}{RT} \quad (3)$$

whereby $p_{tot,i}$ represents the equilibrium pressure. The first pressure difference corresponds to the number of molecules added to the system, while the second pressure difference corresponds to the change of the number of molecules in the gas phase. The total number of molecules adsorbed after i dosing steps, $n_{ads,tot,i}$, is calculated as the sum of the amounts adsorbed in the individual steps. The adsorption isotherm is generated by plotting $n_{ads,tot,i}$ referenced to sample weight or surface area vs. the equilibrium pressure.

Spectra were recorded with a Nicolet Protégé 460 FTIR spectrometer at 4 cm⁻¹ resolution. The pathlength through the cell was 10 mm, so that hydrocarbon gas phase contributions were minimized; for example the Napierian absorbance A_e at a wavelength of 2960 cm⁻¹ (the most intense band of 2,2-dimethylpropane in the analyzed range) was 0.046 at a pressure of 0.94 hPa. However, a background correction of the cell with the gas phase present was recorded for each

step; sample spectra were measured with the specimen in the beam once equilibrium pressure had been reached. All spectra were converted to absorbance and the spectrum obtained of the activated sample in vacuum was subtracted from each spectrum that was acquired during the adsorption experiment. Integration was performed with the OmnicTM software, typically in the range from 3050 to 2650 cm⁻¹ with small adjustments depending on the observed bands.

Determination of integrated molar absorption coefficients is possible using a modified version of the Lambert–Beer law given by Eq. 4.

$$A_e = \kappa c d = \kappa n_{ads,w} \frac{w}{S t} d \quad (4)$$

with A_e the integrated Napierian absorbance in cm⁻¹, κ the integrated Napierian molar absorption coefficient in cm mol⁻¹; c the concentration in mol cm⁻³, d the optical pathlength in cm, $n_{ads,w}$ the adsorbed amount per weight in mol g⁻¹, w the wafer weight in g, S the area of the wafer in cm², t the geometric thickness of the wafer in cm. Eq. 4 can be simplified to give Eq. 5 if it is assumed that the optical pathlength corresponds to the geometric thickness of the wafer:

$$A_e = \kappa n_{ads,w} \frac{w}{S} \quad (5)$$

Results

Molar absorption coefficients of gas phase species

First, gas phase molar absorption coefficients were determined in order to verify the functioning of the pressure measurement and the linearity of the spectral response. *n*-Butane or neopentane was admitted to the cell, and gas phase spectra were recorded at room temperature for various pressures in the hPa range. The spectra were integrated in the C–H stretching region and the area was plotted vs. the gas phase concentration as obtained from the pressure measurement

and the ideal gas law. Linear correlations were obtained, and the slopes were determined by regression. The integrated molar absorption coefficient (κ), which represents an average of the individual coefficients of the various C–H stretching modes,^{3,25,26} was derived from the slope. The results are summarized in Table 1. The observed values match those reported in the literature within a few percent.

Table 1: Gas phase integrated Napierian molar absorption coefficients κ

<i>Molecule</i>	<i>Integration range / cm^{-1}</i>	<i>Pressure range / hPa</i>	<i>R^2 from linear regression</i>	<i>κ_0 measured / $km\ mol^{-1}$</i>	<i>κ from literature* / $km\ mol^{-1}$</i>
<i>n</i> -butane	3050–2750	0.06–9.83	1.000	300	287 ³
neopentane	3050–2650	0.004–89.2	1.000	382	336 ²⁷

*Note: integration range usually encompasses the entire group of C–H stretching bands as in the present paper.

Adsorption isotherms

To verify whether high quality adsorption isotherms could be recorded with the apparatus, *n*-butane was adsorbed on a wafer of H-mordenite. Fig. 1a shows the isotherm up to a pressure of 100 hPa and the inset shows the isotherm in the range 0–4 hPa. This graph demonstrates that the pressure drop method in conjunction with this apparatus delivers good data quality even at low pressures. The adsorbed amounts in each dosing step, which determine the pressure drop, depend on (i) the volumes of the apparatus, which are fixed, (ii) the surface area of sample, which is high for the zeolite with several hundred square meters, and (iii) the absolute amount of sample, which is small with about 20 mg in this experiment. The Lambert–Beer law applies only for a low absorption constant, that is, a low concentration of absorbers or a small absorption coefficient. To

determine the absorption coefficient, it is thus important to be able to collect a sufficient number of data points at low pressures and low coverages.

Fig. 1a)

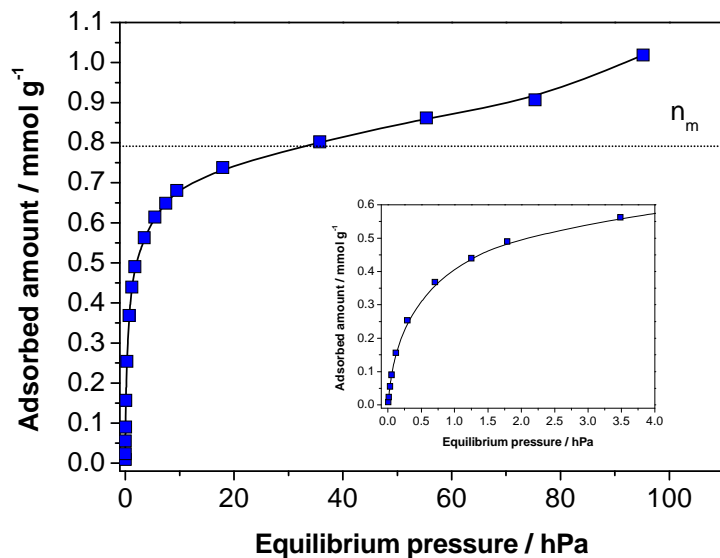


Fig. 1b)

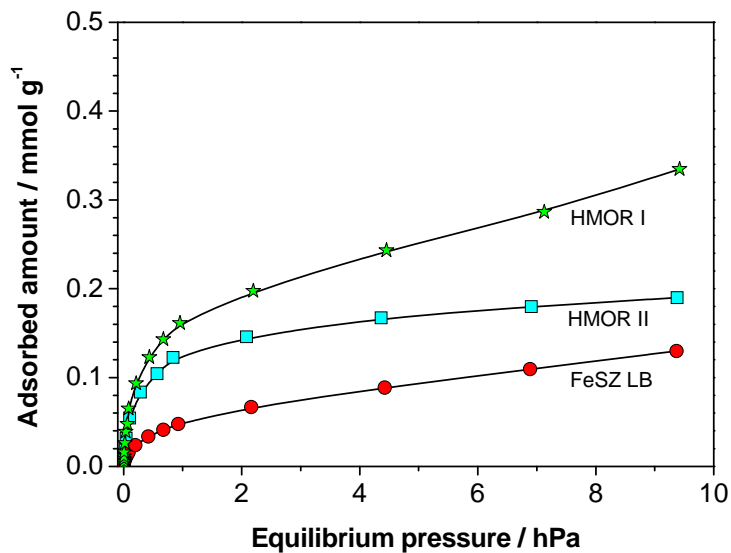


Figure 1: (a) Isotherms of *n*-butane adsorption on H-mordenite I at 297 K; inset low pressure range; (b) Isotherms of neopentane adsorption on H-mordenite I, H-mordenite II and FeSZ LB at 308 K. Samples activated at 723 K in vacuo.

The adsorbed amount varied with the position of the specimen in the cell—in or out of the path of the IR beam. An increase in pressure was observed when moving the wafer into the beam, indicating heating of the specimen by the IR radiation. Accordingly, the isotherm obtained with the wafer in the beam was found to be below that recorded at room temperature. This dependence of the isotherm on the sample position was found to be less pronounced at higher box temperature, and varied with the nature of the adsorbent and the gas. Hence, it seems advantageous to determine IR absorption coefficients in a single experiment, in which the spectra and the adsorbed amount are simultaneously measured.

Neopentane was adsorbed at a nominal (box) temperature of 308 K. Adsorption isotherms for H-mordenite and an iron-promoted sulfated zirconia sample are shown in Fig. 1b. Neopentane uptake was significantly lower than *n*-butane uptake. The neopentane saturation coverage for the two mordenite samples differed. The FeSZ sample was characterized by the smallest uptake per weight.

Molar absorption coefficients of adsorbed species

Spectra were recorded with increasing equilibrium pressure, and the series corresponding to the adsorption isotherms in Fig. 1b are presented in Figs. 2a (FeSZ) and 2b (HMOR-II). There were slight differences in the C–H stretching band positions of neopentane adsorbed on these two catalysts. The strongest band was detected at 2964 cm^{-1} for FeSZ and at 2955 cm^{-1} for H-mordenite. Additional bands towards low frequencies were observed for FeSZ, with the most prominent band at 2822 cm^{-1} . The bands in Fig. 2 were integrated over the entire C–H stretching vibration range. This type of analysis constitutes an averaging of the coefficients of various vibrational modes and of possibly nonequivalent methyl groups after adsorption. However, the

large number of bands and their overlapping makes a discrimination of individual coefficients, which has been demonstrated in other cases,^{11,14} difficult.

Fig. 2a)

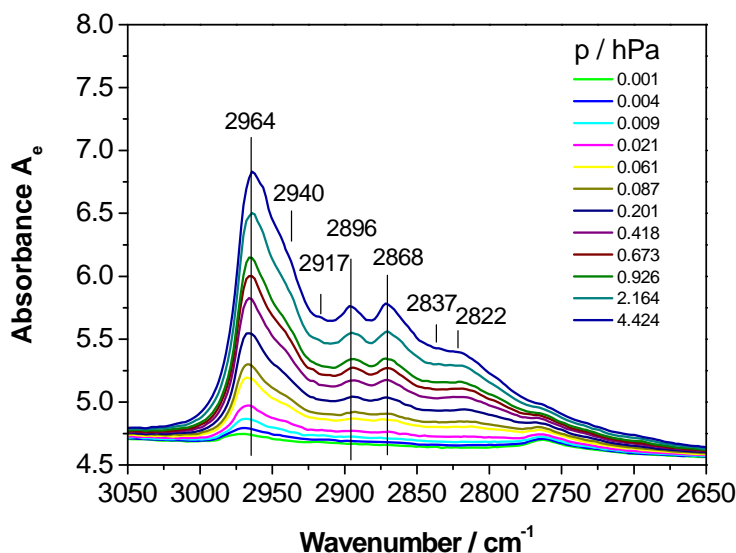


Fig. 2b)

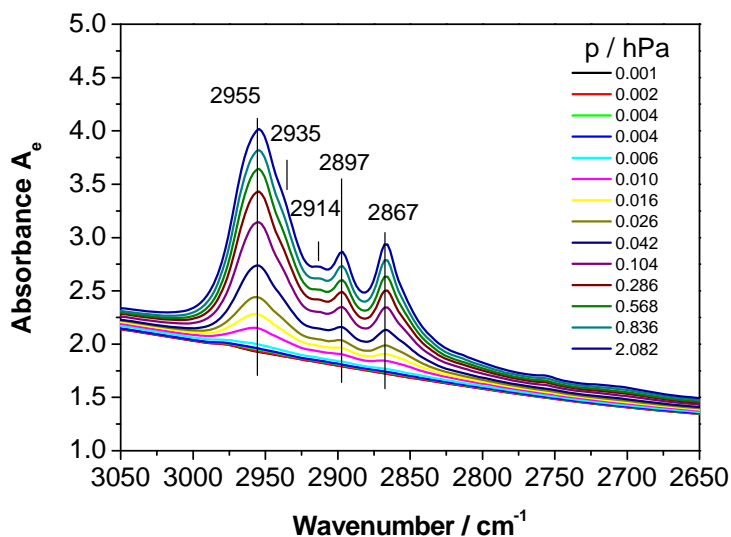


Figure 2: C–H stretching range transmission IR spectra of neopentane adsorbed on (a) iron-promoted sulfated zirconia (FeSZ LB) and (b) H-mordenite II at 308 K; parameter: neopentane equilibrium pressure. Spectra were simultaneously recorded with adsorption isotherms shown in Fig. 1b.

Fig. 3a)

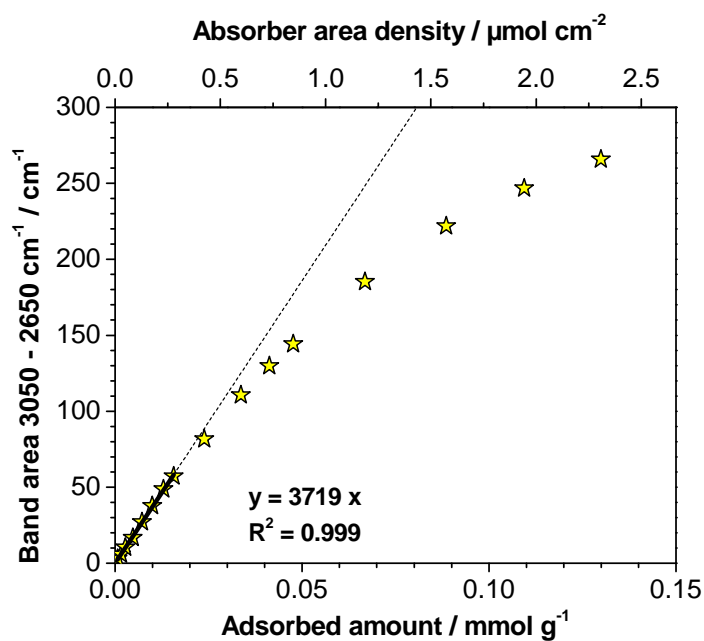


Fig. 3b)

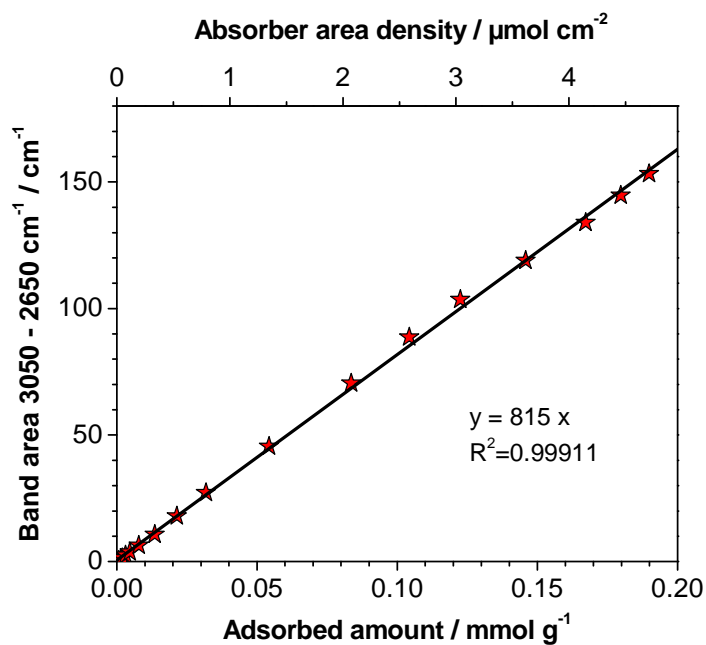


Figure 3: Correlation between integrated Napierian absorbance A_e and coverage of neopentane at 308 K; a) iron-promoted sulfated zirconia (FeSZ LB), b) H-mordenite II. Plots arise from combination of data in Fig. 1b with those in Figs. 2a and 2b.

The obtained integral intensity (from Fig. 2) is plotted as a function of the adsorbed amount (from Fig. 1b) in Fig. 3. At low coverages, an excellent linear relationship is obtained, as indicated by a high correlation coefficient; R^2 was larger than 0.999. The Lambert–Beer law can thus be considered valid under the conditions of the measurement. Linearity of the relation between intensity and coverage was observed at low pressures for a multitude of samples; the linear range varied as can be seen from comparison of Figs. 3a and 3b. Using Eq. 5, values for the integrated molar absorption coefficients κ_ν of C–H stretching vibrations were obtained for a number of zeolitic and sulfated zirconia samples, as listed in Table 2.

Table 2: Apparent Napierian integrated molar absorption coefficients κ_ν for C–H stretching vibrations of neopentane adsorbed at 308 K

<i>Sample</i>	<i>Sieve fraction</i>	<i>Wafer area weight mg cm⁻²</i>	<i>κ_ν km mol⁻¹</i>
HMOR I	unsieved	4.6	595
	unsieved	5.0	860
HMOR II	unsieved	24.8	340
	unsieved	29.7	350
FeSZ LB	unsieved	13.8	2175
	unsieved	17.8	2095
	unsieved	19.4	1945
	d < 20 μm	16.0	1645
FeSZ MB	unsieved	11.1	2125
	unsieved	16.2	2115
	unsieved	22.4	935
FeSZ SB	unsieved	18.6	2660
	unsieved	20.2	2370
SZ LB-1	unsieved	39.5	755
	unsieved	47.2	9015

SZ LB-2	unsieved	31.7	4420
	d < 20 μm	17.2	575
	20 < d < 40 μm	15.0	2660

Surprisingly, different molar absorption coefficients of $728 \pm 187 \text{ km mol}^{-1}$ and $345 \pm 5 \text{ km mol}^{-1}$ were obtained for two H-mordenite samples with similar Si/Al ratio. The first value would suggest an activation of the C–H bonds through adsorption according to our hypothesis, whereas the second value is even slightly lower than the gas phase molar absorption coefficient of $380 \pm 5 \text{ km mol}^{-1}$.

Fig. 4

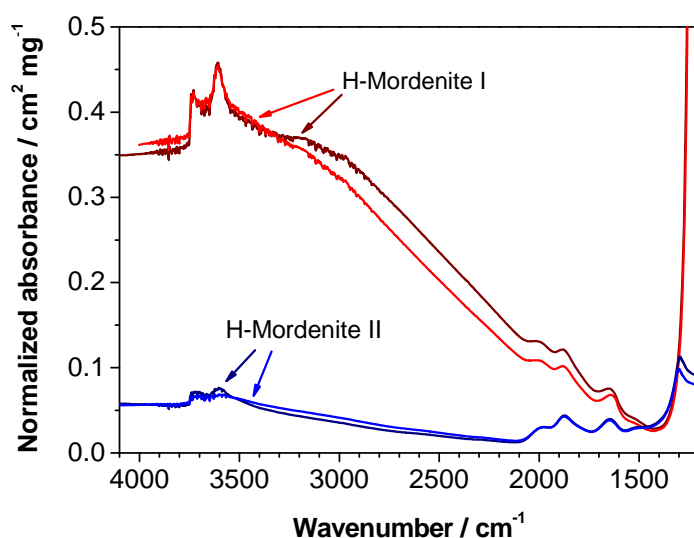


Figure 4: Wafer area weight-normalized transmission IR spectra of two H-mordenite samples. Wafer area weights: 5.0 and 4.6 mg cm^{-1} for Sample I, and 24.8 and 29.7 mg cm^{-1} for Sample II. Samples activated at 723 K in vacuo.

The spectra of these samples were inspected more closely, and Fig. 4, in which the intensities have been normalized to the wafer area weight, reveals that the background contributions differ significantly. The sample producing the higher apparent integrated molar absorption coefficient exhibits a much more pronounced background than the other sample.

Zeolites are insulators and the background in the IR spectra arises mainly from scattering of the radiation by the wafer. Scattering effects become strong when the wavelength and the particle size are similar in dimension, and an increasing background towards higher wavenumbers is typical of many fine catalyst powders. The two samples were investigated by scanning electron microscopy; the images are given in Fig. 5a-c. The sample with the pronounced spectral background consists of smooth crystallites of 100 nm to 2 μm size. The sample producing little background consists of crystallites with an ill-defined shape and a diameter of about 200 nm, which are also agglomerated to larger particles.

Fig. 5: a), b)

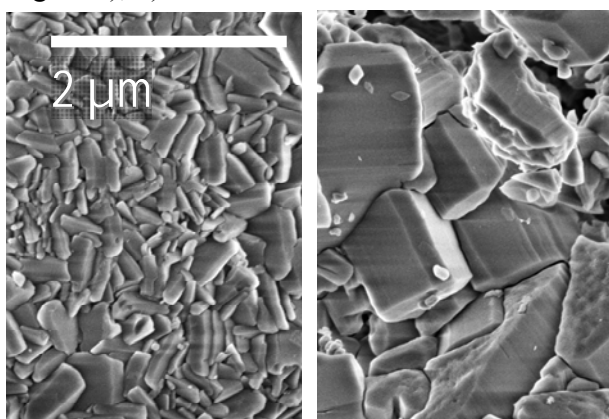


Fig. 5 c)

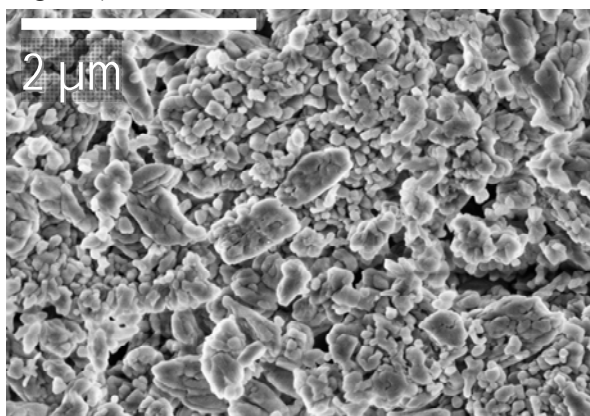


Figure 5: Scanning electron microscopy images of H-mordenites a), b) Sample I and c) Sample II.

The effect of particle morphology on the spectra and the apparent integrated molar absorption coefficients was further investigated by selecting a range of samples with various surface areas and by sieving individual materials into fractions of different particle sizes. The according results are included in Table 2. The apparent integrated molar absorption coefficients for materials of the same chemical composition vary substantially; for example, for neopentane adsorbed on a particular sulfated zirconia, κ_b values between 575 and 4420 km mol⁻¹ were obtained (last three entries in table).

Discussion

Adsorption isotherms

Fig.1 demonstrates that the isotherms have good quality with little scattering of the data points. The correctness of the isotherms is demonstrated through comparison with the literature. The shape of the isotherm for *n*-butane adsorption on H-mordenite (Fig. 1a) with its steep initial increase corresponds to type I according to the IUPAC classification²⁸ and is characteristic of a microporous material. The isotherm was analyzed according to the BET method using a p_0 of 236.5 kPa at 297 K for *n*-butane.²⁹ In the range $p/p_0 = 0-0.015$ the BET plot was linear with $R^2=0.9969$. The linear range is known to be shifted to lower p/p_0 values for microporous materials. The monolayer coverage n_m was determined from the BET plot; the result of 0.79 mmol g⁻¹ corresponds to data given in the literature. The *n*-butane saturation coverage of H-mordenite was reported to be 0.75 mmol g⁻¹ for a sample with Si/Al = 10³⁰ or 0.78 mmol g⁻¹ for a sample with Si/Al = 9.5.³¹

The saturation coverage of neopentane is significantly lower than that of *n*-butane; possible explanations are packing density and pore accessibility. Whereas it was inferred from calculations that branched alkanes are more densely packed in the pores than straight-chain

alkanes,³² experiments show a higher uptake of *n*-alkanes in mordenite in comparison to their branched isomers.³⁰ The difference in saturation coverage between *n*-butane and neopentane is too substantial to be solely attributed to packing density.

The kinetic diameters of neopentane and *n*-butane are 6.2 Å and 4.3 Å,³³ and both molecules fit into the 7.0 Å x 6.5 Å main channels of mordenite. The dimension of the side pockets off the main channels in mordenite is 2.6 x 5.7 Å, which should make them inaccessible to neopentane. There is some debate in the literature as to whether *n*-butane will enter the side pockets. Xu et al.³⁴ reported that of the alkanes only methane can enter, Eder et al.³⁰ stated that the pockets must be “difficult to reach”, Lozano-Castello et al.³¹ proposed *n*-butane could “partially sit” in the side pockets, and van Bokhoven et al.³⁵ reported that mainly sites in the main channels interact with *n*-butane. The significant difference in saturation coverage observed here suggests that a fraction of the pore network that is not accessible to neopentane is at least in part accessible to *n*-butane, and this fraction is probably the side pockets.

The neopentane saturation coverage for the two mordenite samples differed; such variations among samples have been observed before for other adsorptives.³¹ The FeSZ sample was characterized by the smallest uptake, commensurate with its BET surface area of 115 m²/g (vs. several hundred squaremeters for the mordenites).

Molar absorption coefficient measurement - comparison with reported methods and data

A significant number of investigations on molar absorption coefficients address the adsorption of nitrogen bases on solid acids. The interaction of these molecules with surfaces is typically strong, and hence the adsorbed amount can be estimated by assuming complete adsorption after dosing a known amount of vapor. Hughes and White¹⁰ dosed known amounts of pyridine or piperidine onto wafers of HY zeolite, equilibrated for 2.5–3 h, and recorded the

spectra. Various backgrounds were subtracted before the integral intensities were evaluated. Molar absorption coefficients were determined at coverages from 0.03–0.57 mmol g⁻¹. Plots of intensity as a function of coverage show excellent reproducibility and linearity up to an area concentration of 3 μmol cm⁻¹. Emeis¹¹ investigated the adsorption of pyridine on acids such as zeolites and amorphous silica–alumina. Their experiment also involved dosing of known amounts of pyridine. The spectrum of the dehydrated sample was subtracted from the spectrum taken after adsorption. Integral intensities were a linear function of coverage up to about 8 μmol cm⁻¹.

Anderson et al.¹² used a gravimetric experiment to determine the amount of adsorbed pyridine and then conducted IR spectroscopic measurements mimicking the procedure used for the gravimetry. The amount of adsorbed pyridine was adjusted through evacuation at a particular temperature, and measurements at two different temperatures were necessary to derive the absorption coefficients for the two adsorbed pyridine species; however, the data in the paper do not allow conclusions with respect to the linearity of the spectral response.

Thibault-Starzyk et al.¹⁶ integrated a balance into an IR cell and measured the adsorbed amount of pyridine on wafers of HY zeolite via the weight gain. The intensity of the band of the pyridinium ion increased linearly up to a coverage of 8 μmol cm⁻². In a later publication, other authors describe the addition of a basket with more powder into the IR cell to increase the accuracy of the gravimetric measurement in this apparatus.¹⁷

Morterra et al.^{15,36} measured adsorption isotherms with a gas volumetric apparatus; IR spectra were recorded in a separate apparatus in the same pressure range as in the volumetric measurement. Spectroscopic isotherms were generated by integrating the intensities of selected bands and relating them to pressure. When adsorbing CO on TiO₂ samples, a linear correlation between the spectroscopic and the volumetric isotherms was obtained, as manifested by a

constant absorption coefficient over the entire pressure range of 0–100 torr.³⁶ When adsorbing methanol on a variety of silica materials, the two types of isotherm were not parallel except for selected materials, and the authors concluded that the concept of molar absorption coefficients is not generally applicable for species that are physi- or chemisorbed on surfaces.¹⁵

In the present work, a linear correlation between band area and adsorbed amount of neopentane was observed in a wider coverage and absorbance range for zeolitic than for zirconia materials (Fig. 3). The coverage (expressed as absorber area density) ranges exhibiting linearity correspond to those reported in the literature. One pre-requisite for linearity is the uniformity of sites, which can be assumed for the mordenite, whereas the surfaces of sulfated zirconia materials are inhomogeneous.³⁷ The onset of adsorbate–adsorbate interactions could also lead to deviations from linearity at increasing coverages.³⁸ Speaking against these two hypotheses is the fact that the spectral signatures do not vary much with coverage except for a small red shift of the highest frequency band of neopentane adsorbed on FeSZ. (cf. Figs. 2a and b). Linearity could also end when the Lambert Beer law ceases to be valid as the absorption becomes too high. The curve obtained for FeSZ starts to deviate from linearity above an integral intensity (on the basis of A_e) of about 100 cm^{-1} (Fig. 3a); the curve for the zeolite is straight up to about 150 cm^{-1} (Fig. 3b). This difference can be explained with the much higher background intensity of the FeSZ sample (Fig. 2), which moves the absorbance into a range where linearity may no longer be given.

Accuracy of apparent integrated molar absorption coefficients of adsorbed species

Absorption coefficients for two zeolite samples with almost the same chemical composition differed, as did coefficients for various particle size fractions of sulfated zirconia materials. These observations indicate a fundamental problem with the determination of absorption coefficients; this problem must be related to particle size and morphology and thus to scattering effects. The

vastly different backgrounds in Fig. 4 are characteristic for the zeolite morphology and scattering power. Probably, the crystallites in the range of 2 μm size observed for H-mordenite I (Fig. 5b) are responsible for the strong scattering in the range 4000–2000 cm^{-1} (Fig. 4) as their size is close to that of the wavelength (2.5–5.0 μm).

The scattering properties of a wafer are not solely determined by the particle size distribution of the powder, but also by the packing density.³⁹ Indeed, it can be seen in Table 2 that the apparent integrated absorption coefficients are not strictly correlated to wafer area weight. The similarity of the spectra of the same materials in Fig. 4 shows that wafers can be made in a reproducible way when applying the same pressing technique.

To obtain a measure of the scattering power, the transmittance at 4000 cm^{-1} was analyzed. This wavenumber range is close to that of the C–H stretching bands and is devoid of any absorption bands. The transmittance τ through a non-absorbing scattering sample is given by Eq. 6:³⁹

$$\tau \approx \frac{1}{1 + sd} \quad (6)$$

with s the scattering coefficient in cm^{-1} and d the pathlength in cm.

The value of $-\ln(\tau)$ will be called attenuation D_e and not absorbance, as the transmittance is low because of scattering and not because of absorption, and the term attenuation includes the phenomena of luminescence and scattering.⁴⁰ Fig. 6 shows the apparent molar absorption coefficients as a function of the attenuation $D_e(4000)$ for a set of samples. The coefficients were calculated using Eq. (5), which accounts for the specimen thickness d through its area weight, and should be independent of d . However, the apparent integrated molar absorption coefficients of adsorbed neopentane increase with increasing attenuation. This relationship implies that a high scattering power of the specimen leads to a high apparent value of the absorption coefficient. The

observation is consistent with results obtained by Morterra et al.,¹⁵ who found higher apparent absorption coefficients for the C–H stretching vibrations of adsorbed methanol for a more strongly scattering silica (characterized by 60 nm particle diameter) sample in comparison with less strongly scattering silica (15–20 nm). In many cases, attenuation and molar absorption coefficient increase with increasing wafer thickness (Table 2, Fig. 6), as was observed earlier.⁴¹ This result is seemingly inconsistent with earlier reports by Morterra et al.,¹⁵ who found lower apparent molar absorption coefficients with increasing specimen thickness in the range between 6.5 and 39 mg cm⁻¹. However, Morterra worked in a much wider pressure range of 0–60 torr (corresponding to 0–80 hPa) and thus at higher coverages, and, hence, the absorbance was not proportional anymore to the adsorbed amount.

Fig. 6

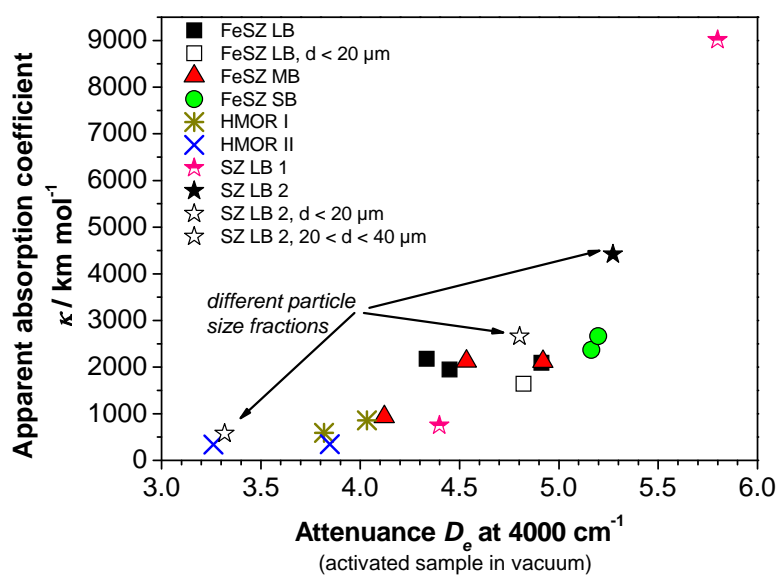


Figure 6: Correlation between apparent molar absorption coefficients and the attenuation at 4000 cm⁻¹ for a variety of sulfated zirconia and zeolite materials. Arrows indicate various particle size fractions from one sulfated zirconia material.

The distribution of the data points in Fig. 6 suggests that some of the assumptions in the data analysis are incorrect. The Lambert–Beer law seems to be valid to the extent that proportionality between absorbance and absorber concentration is fulfilled; however, the optical pathlength also factors into the calculation. To apply the Lambert–Beer law for adsorption on wafers, it had to be modified. In formulating Eq. 5, it is assumed that the optical pathlength d corresponds to the geometric thickness t of the wafer. This assumption will only be true for non-scattering media. Photons that arrive at the detector may have undergone multiple scattering events, resulting in a tortuous path of unknown length. This problem is described in the literature for scattering media such as powders, sintered materials, foams and various types of organic matter.⁴² The optical pathlength d in Eq. 4 can thus be longer than the geometric thickness t , and if that is the case, using the wafer area weight to obtain the coefficients becomes incorrect.

The situation here differs from that reported by Morterra et al.,¹⁵ who suspected that the scattering changes with coverage, and thus no proportionality between adsorbate band intensities and coverage is obtained. Kortüm et al.⁴³ had shown earlier that the presence of adsorbates, for example water, can reduce the scattering coefficient of a powder. Morterra et al.¹⁵ investigated a much wider pressure and thus coverage range than are analyzed in the present work, and, for these greater ranges, variation of the scattering ability may indeed have to be taken into account.

Fig. 6 shows how scattering effects lead to excessive values for the molar absorption coefficients. The question arises as to whether the true absorption coefficients can be estimated through extrapolation of the molar absorption coefficient to zero attenuation. With the data collected so far, one would have to extrapolate very far on the basis of few data points and the result would likely be inaccurate.

The preceding discussion shows that it is very difficult to accurately measure IR absorption coefficients for adsorbates on strongly scattering samples and casts doubt on the frequently made

assumption that quantification is easily possible when working in transmission geometry. The problem can be circumvented by investigating materials that do not scatter strongly or by resorting to bands that are in regions of the spectrum that are not affected by scattering. A series of cation-exchanged Y-zeolites proved to be suitable, and it was possible to determine the molar absorption coefficients for the C–H stretching vibrations of adsorbed ethane⁴¹ and for the C–H and C=C vibrations of adsorbed propene.⁴⁴ An important application that could be affected by scattering problems is the determination of the number of Brønsted and Lewis acid sites on solid acid catalysts through adsorption of pyridine. Fortunately, the analyzed bands of pyridine are in a wavenumber regime where scattering is often not particularly strong. Still, scattering coefficients depend on particle size, and comparison of samples with largely different surface areas, for example, may not be possible. Moreover, several authors report variations in absorption coefficients depending on the nature of the surface,^{13,41,44,45} which in turn depends on materials composition and activation conditions. These observations suggest that IR absorption coefficients of adsorbed molecules are not transferable from one adsorbent to another.

Conclusions

Transmission IR spectra and adsorption isotherms were simultaneously acquired to follow the adsorption of small hydrocarbons on solid acids such as zeolites and sulfated zirconia materials. The intensity of the C–H stretching vibrations of 2,2-dimethylpropane was proportional to the adsorbed amount in the range of low coverages (up to 0.02 or 0.2 $\mu\text{mol g}^{-1}$, depending on the sample). However, the molar absorption coefficients determined from the slopes of these correlations were found to be overestimated because of scattering effects.

The frequently made assumption that transmission IR spectra are easily quantified neglects that the transmitted radiation is only a correct representation of the absorbed radiation in the

absence of phenomena such as scattering or reflection. Scattering can be strong in self-supporting wafers of fine catalyst powders, which renders the determination of accurate values of absorption coefficients for adsorbate vibrations difficult. In turn, the measurements of the number of sites, for examples acid sites, by means of IR spectroscopy and absorption coefficients from the literature may easily be falsified through scattering. Only if scattering is absent or minimized, molar absorption coefficients may be determined or applied.

Acknowledgements

The help of Sabine Wrabetz, Annette Trunschke, and Jörg Wagatha in designing and assembling the vacuum and gas dosing apparatus for IR spectroscopy is appreciated. Gisela Weinberg is acknowledged for recording the SEM images, Fritz Fetting and Johannes A. Lercher for providing the zeolite samples I and II, and Robert Schlögl for supporting the project. Funding was provided by Deutsche Forschungsgemeinschaft grants JE 267/2-1 and RUS 113/788/0-1, and the Max Planck Society.

References

1. Zaki, M. I.; Knözinger, H. An Infrared-Spectroscopy Study of Carbon Monoxide Adsorption on α -Chromia Surfaces: Probing Oxidation States of Coordinatively Unsaturated Cations. *J. Catal.* **1989**, *119*, 311–321.
2. Knözinger, H.; Huber, S. IR spectroscopy of Small and Weakly Interacting Molecular Probes for Acidic and Basic Zeolites. *J. Chem. Soc., Faraday Trans.* **1998**, *94*, 2047–2059.
3. Gussoni, M.; Castiglioni, C. Infrared intensities. Use of the CH-Stretching Band Intensity as a Tool for Evaluating the Acidity of Hydrogen Atoms in Hydrocarbons. *J. Molec. Struc.* **2000**, *521*, 1–18.

4. Kazansky V. B.; Serykh A. I.; Pidko E. A. DRIFT Study of Molecular and Dissociative Adsorption of Light Paraffins by HZSM-5 Zeolite Modified with Zinc Ions: Methane Adsorption. *J. Catal.* **2004**, *225*, 369–373.
5. Kazansky, V. B.; Subbotina, I. R.; Pronin, A. A.; Schlögl, R.; Jentoft, F. C. Unusual Infrared Spectrum of Ethane Adsorbed by Gallium Oxide. *J. Phys. Chem. B* **2006**, *110*, 7975–7978.
6. Kazansky, V. B.; Subbotina, I. R.; Jentoft, F. C. Intensities of Combination IR Bands as an Indication of the Concerted Mechanism of Proton Transfer from Acidic Hydroxyl Groups in Zeolites to the Ethylene Hydrogen-Bonded by Protons. *J. Catal.* **2006**, *240*, 66–72.
7. Kazansky, V. B., Subbotina, I. R.; Jentoft, F. C.; Schlögl, R. Intensities of C-H IR Stretching Bands of Ethane and Propane Adsorbed by Zeolites as a New Spectral Criterion of Their Chemical Activation via Polarization Resulting from Stretching of Chemical Bonds. *J. Phys. Chem. B* **2006**, *110*, 17468–17477.
8. Risse, T; Carlsson, A.; Bäumer, M.; Klüner, T.; Freund, H.-J. Using IR Intensities as a Probe for Studying the Surface Chemical Bond. *Surf. Sci.* **2003**, *546*, L829–835.
9. Platon, A.; Thomson, W. J. Quantitative Lewis/Brønsted Ratios Using DRIFTS. *Ind. Eng. Chem. Res.* **2003**, *42*, 5988–5992.
10. Hughes, T. R.; White, H. M. A Study of the Surface Structure of Decationized Y Zeolite by Quantitative Infrared Spectroscopy. *J. Phys. Chem.* **1967**, *71*, 2192–2201.
11. Emeis, C. A. Determination of Integrated Molar Extinction Coefficients for Infrared Absorption Bands of Pyridine Adsorbed on Solid Acid Catalysts. *J. Catal.* **1993**, *141*, 3437–354.

12. Anderson, J. A.; Fergusson, C.; Rodríguez-Ramos, I.; Guerrero-Ruiz, A. Influence of Si/Zr Ratio on the Formation of Surface Acidity in Silica-Zirconia Aerogels. *J. Catal.* **2000**, *192*, 344–353.
13. Sievers, C.; Onda, A.; Olindo, R.; Lercher, J. A. Adsorption and Polarization of Branched Alkanes on H-LaX. *J. Phys. Chem. C* **2007**, *111*, 5454–5464.
14. Pieta, I. S.; Ishaq, M.; Wells, R. P. K.; Anderson, J. A. Quantitative Determination of Acid Sites on Silica–Alumina. *Appl. Catal. A: General* **2010**, *390*, 127–134.
15. Morterra, C.; Magnacca, G.; Bolis, V. On the Critical Use of Molar Absorption Coefficients for Adsorbed Species: The Methanol/Silica System. *Catal. Today* **2001**, *70*, 43–58.
16. Thibault-Starzyk, F.; Gil, B.; Aiello, S.; Chevreau, T.; Gilson, J.–P. In Situ Thermogravimetry in an Infrared Spectrometer: An Answer to Quantitative Spectroscopy of Adsorbed species on Heterogeneous Catalysts. *Microp. Mesop. Mater.* **2004**, *67*, 107–112.
17. Vimont, A.; Travert, A.; Binet, C.; Pichon, C.; Mialane, P.; Sécheresse, F.; Lavalley, J.–C. Relationship between Infrared Spectra and Stoichiometry of Pyridine- $\text{H}_3\text{PW}_{12}\text{O}_{40}$ Salts Using a new TGA-Infrared Coupling. *J. Catal.* **2006**, *241*, 221–224.
18. Hino, M.; Kobayashi, S.; Arata, K. Solid Catalyst Treated with Anion: 2. Reactions of Butane and Isobutane Catalyzed by Zirconium Oxide-Treated with Sulfate Ion – Solid Superacid Catalyst. *J. Am. Chem. Soc.* **1979**, *101*, 6439–6441.
19. Essayem, N.; Ben Taârit, Y.; Feche, C.; Gayraud, P. Y.; Sapaly, G.; Naccache, C. Comparative Study of *n*-Pentane Isomerization Over Solid Acid Catalysts, Heteropolyacid, Sulfated Zirconia, and Mordenite: Dependence on Hydrogen and Platinum Addition. *J. Catal.* **2003**, *219*, 97–106.

20. Fogash, K. B.; Hong, Z.; Dumesic, J. A. Effects of Isobutylene on Isobutane Isomerization over H-Mordenite. *J. Catal.* **1998**, *173*, 519-529.
21. Adeeva, V.; de Haan, J. W.; Jänchen, J.; Lei, G. D.; Schünemann, V.; van de Ven, L. J. M.; Sachtler, W. M. H.; van Santen, R. A. Acid Sites in Sulfated and Metal-Promoted Zirconium Dioxide Catalysts. *J. Catal.* **1995**, *151*, 364–372.
22. Cheung, T.-K.; d'Itri, J. L.; Lange, F. C.; Gates, B. C. Neopentane Cracking Catalyzed by Iron-Promoted and Manganese-Promoted Sulfated Zirconia. *Catal. Lett.* **1995**, *31*, 153–163.
23. Hahn, A.; Ressler, T.; Jentoft, R. E.; Jentoft, F. C. The Role of the 'Glow Phenomenon' in the Preparation of Sulfated Zirconia Catalysts. *Chem. Comm.* **2001**, 537–538.
24. Hahn, A. H. P.; Jentoft, R. E.; Ressler, T.; Weinberg, G.; Schlögl, R.; Jentoft, F. C. Rapid Genesis of Active Phase during Calcination of Promoted Sulfated Zirconia Catalysts. *J. Catal.* **2005**, *236*, 324–334.
25. Francis, S. A. Absolute Intensities of Characteristic Infra-Red Absorption Bands of Aliphatic Hydrocarbons. *J. Chem. Phys.* **1950**, *18*, 861–865.
26. Wexler, A. S. Infrared Determination of Structural Units in Organic Compounds by Integrated Intensity Measurements: Alkanes, Alkenes and Monosubstituted Alkyl Benzenes. *Spectrochim. Acta* **1965**, *21*, 1725–1742.
27. Stal'makhova, I. P.; Finkel' A. G.; L. M. Sverdlov Experimental and Theoretical Study of the Absolute Intensities of Infrared Spectra of Branched Paraffinic Hydrocarbons. *J. Appl. Spectroscopy* **1969**, *11*, 809–813.
28. Sing, K. S. W.; Everett, D. H.; Haul, R. A. W.; Moscou, L.; Pierotti, R. A.; Rouquérol, J.; Siemieniowska, T. Reporting Physisorption Data for Gas Solid Systems with Special

Reference to the Determination of Surface Area and Porosity (Recommendations 1984) *Pure & Appl. Chem.* **1985**, *57*, 603–619.

29. CRC Handbook of Chemistry and Physics, 67th Ed., CRC Press, Boca Raton, 1986–1987.
30. Eder, F.; Stockenhuber, M.; Lercher, J. A. Sorption of Light Alkanes on H-ZSM5 and H-mordenite. *Stud. Surf. Sci. Catal.* **1995**, *97*, 495–500.
31. Lozano-Castello, D.; Zhu, W.; Linares-Solano, A.; Kapteijn, F.; Moulijn, J. A. Micropore Accessibility of Large Mordenite Crystals. *Micropor. Mesopor. Mater.* **2006**, *92*, 145–153.
32. van Baten, J.M.; Krishna, R. Entropy Effects in Adsorption and Diffusion of Alkane Isomers in Mordenite: An Investigation Using CBMC and MD Simulations. *Microporous and Mesoporous Materials* **2005**, *84*, 179–191.
33. Breck, D. W. Zeolite Molecular Sieves: Structure, Chemistry, and Use, John Wiley & Sons, New York, 1974.
34. Xu, Q.; Eguchi, T.; Nakayama, H.; Nakamura, N. Proton Magnetic Resonance of C_nH_{2n+2} ($n = 1-4$) Adsorbed in Mordenite: Dynamic Behaviour and Host-Guest Interaction. *J. Chem. Soc. Faraday Trans.* **1996**, *92*, 1039–1042.
35. van Bokhoven, J. A.; Tromp, M.; Koningsberger, D.C.; Miller, J.T.; Pieterse, J. A. Z.; Lercher, J. A.; Williams, B.A.; Kung, H.H. An Explanation for the Enhanced Activity for Light Alkane Conversion in Mildly Steam Dealuminated Mordenite: The Dominant Role of Adsorption. *J. Catal.* **2001**, *202*, 129–140.
36. Morterra, C.; Garrone, E.; Bolis, V.; Fubini, B. An Infrared Spectroscopic Characterization of the Coordinative Adsorption of Carbon Monoxide on TiO_2 . *Spectrochim. Acta* **1987**, *43A*, 1577–1581.

37. Kim, S. Y.; Goodwin Jr., J. G.; Galloway, D. *n*-Butane Isomerization on Sulfated Zirconia: Active Site Heterogeneity and Deactivation. *Catal. Today* **2000**, *63*, 21–32.
38. Rosenberg, D. J.; Bachiller-Baeza, B.; Dines, T. J.; Anderson, J. A. Nature of Surface Sulfate Species and the Generation of Active Sites on Silica-Zirconia Mixed-Oxide Catalysts. *J. Phys. Chem. B* **2003**, *107*, 6526–6534.
39. Kortüm, G. *Reflectance Spectroscopy*, Springer **1969**, p. 121–121.
40. <http://goldbook.iupac.org/A00513.html>; accessed June 12, 2012.
41. Subbotina, I. R.; Kazansky, V. B.; Kröhnert, J.; Jentoft, F. C. Integral Absorption Coefficients of C–H Stretching Bands in IR Spectra of Ethane Adsorbed by Cationic Forms of Y Zeolite. *J. Phys. Chem. A* **2009**, *113*, 839–844.
42. Sjöholm, M.; Somesfalean, G.; Alnis, J.; Andersson-Engels, S.; Svanberg, S. Analysis of Gas Dispersed in Scattering Media. *Optics Letters* **2001**, *26*, 16-18.
43. Kortüm, G., Braun, W., Herzog, G., Prinzip und Meßmethodik der Diffusen Reflexionsspektroskopie. *Angew. Chem.* **1963**, *75*, 653–661; *Angew. Chem. Int. Ed.* **1963**, *2*, 333–341.
44. Subbotina, I. R.; Kazansky, V. B.; Jentoft, F. C.; Schlögl, R. IR Extinction Coefficients as a Criterion for Chemical Activation upon Adsorption: Propene Interaction with Cationic Forms of Y Zeolite. *Zeolites and Related Materials: Trends, Targets and Challenges*, Proceedings of 4th International FEZA Conference, Eds. A. Gedeon, P. Massiani, F. Babboneau, *Stud. Surf. Sci. Catal.* **2008**, *174B*, 849–852.
45. Rosenberg, D. J.; Anderson, J. A. On Determination of Acid Site Densities on Sulfated Oxides. *Catal. Lett.* **2002**, *83*, 59–63.

Table of Contents Graphic

